Estimation of Pollutant Load in Typical Drainage Ditches of Ningxia Yellow River Diversion Irrigation Area Based on LOADEST Statistical Model

Xiuxia Ma [1], Wenfa Peng [2], Bingwei Tong [1], Taiyun Li [1], Le Wang [1], Bin Du [1] and Chaochao Li [2,*]

[1] Ningxia Institute of Water Resources Research, Yinchuan 750021, China; maxiuxiast@163.com (X.M.); tongbw1976@126.com (B.T.); ltaiyunsky@163.com (T.L.); wangle753400@163.com (L.W.); nddubin@163.com (B.D.)

[2] School of Civil and Hydraulic Engineering, Ningxia University, Yinchuan 750021, China; pengwenfa1006@163.com

* Correspondence: lichaochao@nxu.edu.cn

Abstract: To comprehensively comprehend the spatiotemporal variations in pollution load within the Sixth Drainage Ditch of the Ningxia Yellow River Diversion Irrigation Area, we employed the LOADEST model. We utilized daily flow data and concentrations of ammonia nitrogen (NH_3-N), nitrate nitrogen (NO_2-N), total nitrogen (TN), and total phosphorus (TP) to construct regression equations for the pollutant load at four distinct monitoring sections of the Sixth Drainage Ditch. The results unveiled an impressive range of correlation coefficients (R^2) for the pollution load regression equations at the four monitoring sections, ranging from 72.42% to 94.4%. This indicates a strong fit for the pollution load regression equations, rendering them suitable for estimating the pollution load of the Sixth Drainage Ditch. Furthermore, the changing patterns of various pollutants in the same monitoring section exhibit a remarkable level of consistency. In each case, they initially experience an upward trajectory followed by a subsequent decrease. Notably, the total nitrogen (TN) load in the drainage area exceeds that of the total phosphorus (TP). The spatial distribution patterns of the total nitrogen (TN) and total phosphorus (TP) load within the Sixth Drainage Ditch exhibit a progressive increase from the upstream to downstream areas. Meanwhile, the spatial distribution characteristics of ammonia nitrogen (NH_3-N) and nitrate nitrogen (NO_2-N) follow a similar pattern of an initial increase followed by a decrease.

Keywords: LOADEST model; Ningxia diversionary yellow irrigation district; pollutant load; drainage ditch; spatiotemporal variation

1. Introduction

Water is a crucial resource for human survival and progress. However, water pollution has evolved into a global environmental challenge, significantly impacting the economic and social development of nations, and the health of people [1]. The deterioration in water environments is a result of the interplay between point source pollution and non-point source pollution. In recent years, with the increasing prominence of water environmental issues and a relatively higher level of control over point source pollution, there is a growing focus and recognition of non-point source pollution. This is particularly evident in concerns about agricultural non-point source problems arising from the widespread use of fertilizers and pesticides [2]. Agricultural non-point source pollution encompasses a range of pollutants stemming from agricultural production activities. These pollutants diffuse from the soil environment into water bodies at low concentrations over a wide area, primarily through mechanisms such as surface runoff, drainage, and subsurface seepage within farmland. The regions of the Yellow River in China most severely affected by pollution are concentrated primarily in the upper reaches of Ningxia, Inner Mongolia, and the middle

reaches of Yuguan. This critical issue is exacerbated not only by the centralized discharge of industrial and urban wastewater, sewage, and other point source pollutants but also by significant contributions from agricultural non-point source pollution factors. These include factors such as changes in irrigation practices and soil erosion, all of which have become pivotal factors influencing water pollution in the Yellow River [3]. This dual role of agriculture as both a 'victim' and 'contributor' to water pollution is evident. On the one hand, water pollution negatively impacts the water quality of irrigated farmlands. On the other hand, it triggers reactions between nitrogen and phosphorus nutrients in irrigation drainage, thereby compounding the repercussions of water pollution. Due to the diffuse, erratic, inconspicuous, and delayed nature of agricultural non-point source pollution, addressing non-point sources originating from agriculture has emerged as a formidable challenge in the realm of environmental pollution control [4].

Prominent agricultural non-point source pollution load models in use today encompass the SoilWater and Assessment Tools (SWAT), Continuous agricultural non-point source pollution model (AnAGNPS), Chemicals, Runoff, and Erosion from Agricultural Management Systems (CREAMS), Hydrological Simulation Program-Fortran (HSPF), and several others [5]. Of these models, the SWAT model sees widespread application in China. However, its operational requirements involve a multitude of parameters and various monitoring data inputs, often posing challenges due to the dearth of continuous and complete measured data in practice [6]. In response, the United States Geological Survey has developed the LOADEST pollutant flux estimation model, coded in Fortran. This innovative model effectively leverages continuous daily flow data and limited, discrete water quality data to establish corresponding pollutant flux regression equations, allowing for the estimation of pollutant transport flux at various time scales in rivers [7]. Beyond its fundamental utility in load estimation, the LOADEST model offers versatile applications: optimizing water quality monitoring frequency, evaluating the implementation efficacy of Best Management Practices (BMPs), and serving as a valuable tool for parameter calibration and validation in pollutant migration and transformation mechanism models. Such applications significantly enhance the precision of mechanism models, offering a nuanced understanding of water quality dynamics [8]. The LOADEST model is characterized by its resource-efficiency and exceptional accuracy, gradually gaining ground in the realm of water pollution load prediction and being widely adopted in multiple global regions [9]. For instance, Pointer et al. [10] harnessed the LOADEST model to simulate the nitrogen load in the North Carolina Reservoir, while Duan [11] employed LOADEST to analyze phosphorus load variations from urban to rural areas in Chesapeake Bay. Robert et al. [12] set the LOADEST statistical model to study seasonal and annual fluxes of organic pollutants in the Arctic Ocean and its surrounding waters, a study of great significance for marine pollution control in the Arctic region. Toomas et al. [13] employed the LOADEST statistical model to examine dissolved organic carbon (DOC) pollution loads in shallow lakes. Li et al. [8] used the LOADEST model to establish regression equations for pollutant flux and subsequently estimate river inflow flux and water quality from 1999 to 2008, offering a simplified and data-efficient approach to estimating pollutant flux in rivers with infrequent water quality monitoring. In addition, their findings provide a scientific basis for basin-wide total load control. Meng et al. [14] harnessed the capabilities of the LOADEST model to develop a statistical regression model linking pollutant flux to river flow. They utilized hydrological and water quality data collected from the Huai River as it flowed into Hongze Lake between 2015 and 2020. This analysis enabled them to accurately estimate the pollutant flux of both the TN and TP entering Hongze Lake via the Huai River. Wang et al. [15] applied the LOADEST model to simulate the total runoff and nitrogen and phosphorus output flux processes of the Simao River, further estimating the contribution of nitrogen and phosphorus output from the base flow.

Nestled in the arid expanse of northwestern China, the Ningxia Hui Autonomous Region grapples with an acute scarcity of water resources, with per-capita availability languishing at less than one-third of the national average. This places Ningxia among

the country's most water-challenged provinces [16]. The region's economic development primarily hinges on the utilization of Yellow River water as a vital resource. In July 2020, General Secretary Xi Jinping conducted an inspection of Ningxia, bestowing upon it the significant responsibility of establishing itself as a 'pioneering area for ecological protection and high-quality development within the Yellow River Basin.' This role carries immense importance in preserving the ecological security of the Yellow River Basin [17]. In recent years, the rapid expansion of the breeding industry in Ningxia has given rise to challenges such as unsustainable irrigation practices and the excessive use of nitrogen fertilizers. These have emerged as significant sources of pollution, causing harm to the soil and water environment in the region [18]. While there has been some improvement, with Class IV and lower water quality now accounting for 45.9% of the monitored sections within the core channels [19], it is evident that water quality management and protection continue to confront substantial hurdles. The contamination of water quality by drainage channels has exacerbated water pollution in the Yellow River, jeopardizing the safety of water quality in the river's main stem and posing threats to the ecological equilibrium of the irrigated areas. This situation stands in stark contrast to our district's ecological development strategy and the prerequisites for the high-quality development of the Yellow River.

To gain a more profound understanding of the water environment quality in the Ningxia Yellow River Irrigation Area, we have selected the Sixth Drainage Ditch as our research focus. The LOADEST statistical model is primarily employed for estimating the nitrogen and phosphorus pollutant loads in agricultural runoff. Through a systematic spatiotemporal analysis, our commitment is to unveil the patterns of variation in the pollutant loads within the Sixth Drainage Ditch, utilizing the available limited data. Our objective is to provide a comprehensive and in-depth foundation of data and theoretical support for the improvement in water environment quality in the Ningxia Yellow River Irrigation Area. Additionally, we aim to offer a more streamlined and efficient methodology for the study of pollutants in agricultural runoff.

2. Materials and Methods

2.1. Study Area

The Sixth Drainage Ditch, nestled within the Ningxia Yellow River Irrigation Area, is located in Shizuishan City, Ningxia. It originates from Shaojiaqiao Village in Headgate Town, Pingluo County, Shizuishan City, Ningxia, winding its way northward until it merges with the Fifth Drainage Ditch in Weizha Town, Huinong District, Shizuishan City, Ningxia. The entire stretch of the ditch spans a length of 28.71 km, with the segment traversing Pingluo encompassing 19.7 km. The overall drainage area of the Sixth Drainage Ditch covers 113 square kilometers, and the Pingluo section spans 40 square kilometers. At the boundary between Pingluo and Huinong, the designed flow rate is 3.42 m^3/s. The measured maximum flow rate stands at 4.25 m^3/s, with a multi-year average flow rate of 2.45 m^3/s. The multi-year average drainage volume measures at 1.049×10^7 m^3, featuring an average gradient of 1/4500. This drainage ditch courses through several villages, including Yumin Village and Waihonggang Village in Touzha Town, as well as Guangming Village, Shengli Village, Tianjia Village, Dongrun Village, Xiling Village, Lingsha Village, Hejia Village, and Xianfeng Village in Lingsha Township. Baofeng Town comprises 14 villages from 3 townships, encompassing Zhongfang Village, Quyang Village, Xinqu Village, and Majiaqiao Village. The ditch maintains a width ranging from 10 to 15 m. The Sixth Drainage Ditch exhibits relatively modest water volume, with no water flow detected in the initial 4 km of the ditch. Around 3 km north of Yumin Village's third team, water flow begins, though the majority of the ditch sections feature shallow depths and limited mobility. The first 4 km of the ditch are adorned with reeds and other aquatic vegetation, with certain sections showcasing small aquatic plant populations. Forest belts are notably absent along most of the ditch's banks. The villages adjacent to the ditch lack sewage collection pipe networks or sewage treatment facilities, do not have direct outlets for domestic sewage, and house no industrial enterprises or associated industrial

wastewater sources. Approximately 500 m east of Team 7 in Guangming Village, there exists a poultry breeding facility, suspected to have a sewage outlet, and the water quality in the nearby section of the breeding farm's ditch exhibits slight discoloration. Based on water quality monitoring data from 2021, the water quality within the Sixth Drainage Ditch corresponds to II~Class III. This ditch comprises a total of 25 branch and bucket ditches, 39 agricultural ditches, boasting an aggregate length of 22.7 km, and is equipped with 15 bridges, 1 culvert, and 22 tailwater outlets. For the precise geographical location of the Sixth Drainage Ditch within the Ningxia Yellow River Diversion Irrigation Area, please refer to Figure 1.
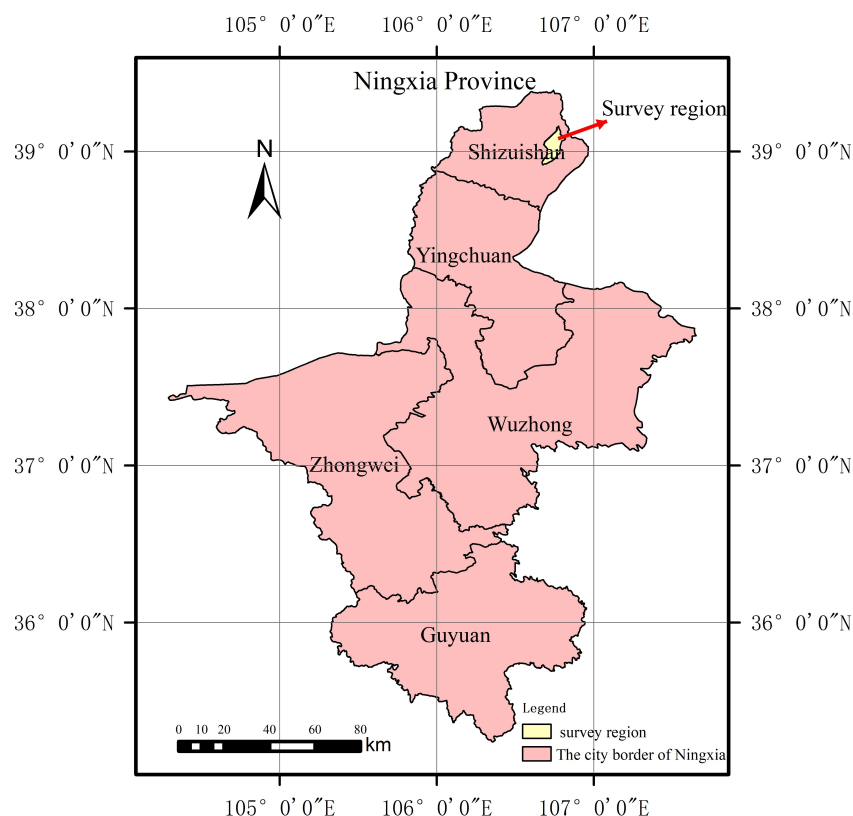

Figure 1. Geographical location of the Sixth Drainage Canal in the Yellow River Irrigation Area of Ningxia.

2.2. Source of Data

As depicted in Figure 2, this study designated four control sections along the course of the Sixth Drainage Ditch. Over the period spanning 2021 to 2022, water samples were routinely collected from these monitoring sites, typically once or twice each month, for comprehensive testing. The primary focus of the tests encompassed critical parameters such as TN, TP, NH_3-N, and NO_2-N. Considering the water irrigation cycle in agriculture, there was limited drainage from farmland in January–April, September, and December 2021, making it challenging to effectively monitor pollutant concentrations in the water. Therefore, only data from the remaining six months were included in the pollution concentration statistics. These monitoring sections have been designated as M1, M2, M3, and M4, with flow data sourced directly from measurements provided by the local hydrological bureau.
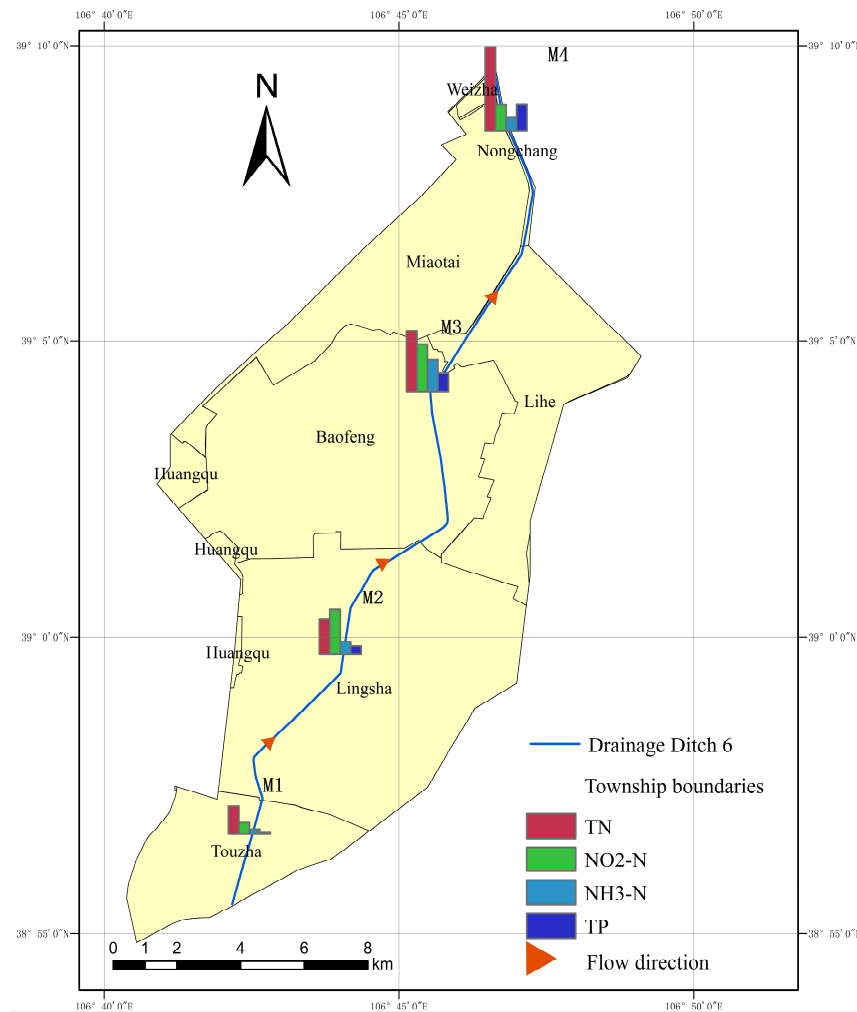
Figure 2. Locations of control sections.

2.3. LOADEST Model

The LOADEST model comprises two principal modules: the input module and the output module. The input module includes control files, source files, calibration files, and estimation files, while the output module encompasses corresponding files, auxiliary files, residual files, and load calculation files [20]. LOADEST effectively harnesses limited and discrete flow and water quality data to create regression equations that correlate with pollutant fluxes. Subsequently, it estimates the transport fluxes of various pollutants at diverse time scales in river systems [21]. Recognizing the diverse diffusion patterns of pollutants and their varying responsiveness to river dynamics, the LOADEST model offers users a choice among 11 regression models. Model equation parameters are estimated via methods such as maximum likelihood estimation, modified maximum likelihood estimation, and minimum absolute deviation [22]. The degree of fit for the chosen model equation is assessed by the coefficient R^2, with a higher R^2 value approaching 1 indicating a stronger and more accurate fit [23].

The fundamental principle underpinning the estimation of pollutant flux through the LOADEST water quality model is articulated as follows [21]:

$$\hat{L}_\tau = \Delta t \sum_{i=1}^{NP} \left(\hat{QC} \right)_i = \Delta t \sum_{i=1}^{NP} \hat{L}_i \tag{1}$$

In the equation, $\hat{L}_i$ represents the instantaneous pollutant load (kg/month); $\hat{L}_\tau$ represents the pollutant load over a τ time period (kg/month); Δt represents the time interval;

NP represents the number of discrete time intervals; *C* represents the instantaneous water quality (mg/L); *Q* represents the time-averaged flow (m^3/month).

3. Results

3.1. Characteristics of Flow and Pollutant Concentration Variation in the Main Monitoring Sections of the Sixth Drainage Ditch

Figure 3 offers a comprehensive view of the dynamic shifts in flow and pollutant concentrations across the four monitoring sections within the Sixth Drainage Ditch. As depicted in the figure, the highest flow levels occur during the months of June and July, predominantly attributed to the extensive irrigation practices in the region. The M1 monitoring section, positioned upstream of the Sixth Drainage Ditch, encompasses a relatively smaller controlled drainage area, resulting in a correspondingly reduced flow rate. This section exhibits two distinct peaks during the spring and summer irrigation period, spanning from May to September. The first peak materializes in mid-June, with a subsequent peak in late July. During the winter irrigation phase in October and November, the flow in this section further diminishes, and the flow pattern remains relatively consistent. The flow patterns for the middle section monitoring sections, M2 and M3, bear a close resemblance. These sections exhibit two peaks during the spring and summer irrigation period, marked by a sharp initial peak followed by a shorter and broader second peak. This phenomenon primarily arises from the widespread and lengthy irrigation practices that characterize the entire drainage area. In the downstream M4 monitoring section, the flow pattern indicates that from mid-June to the end of August, the flow in this section consistently registers at lower levels than that of M3. This variation predominantly stems from the presence of numerous pump stations along the channel, which are integral to the recycling of drainage water. The annual flow dynamics across the four monitoring sections within the Sixth Drainage Ditch display periodic fluctuations, featuring three notable peaks. Of particular significance are the peaks in June and July, coinciding with the crop growth season in the irrigation district. During this period, agricultural activities, such as field irrigation and fertilization, occur frequently.
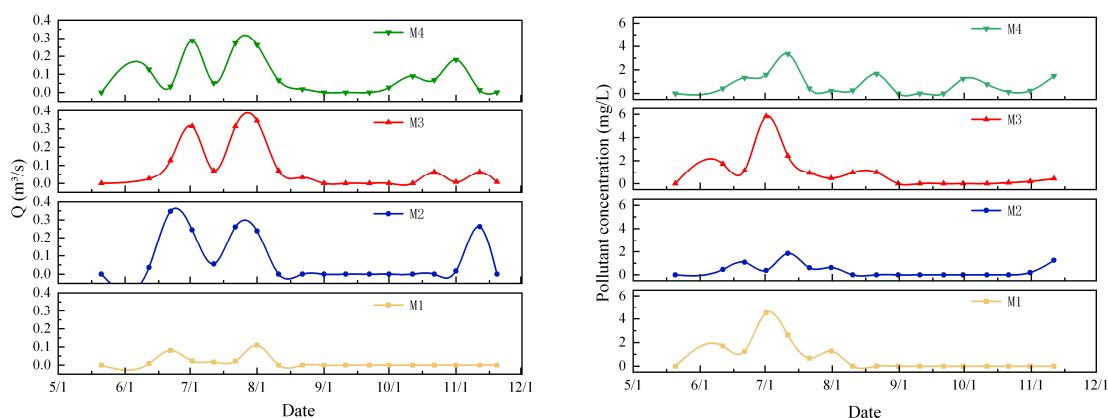

Figure 3. The flow and concentration variations of the four monitoring sections of the Sixth Drainage Canal.

With the conclusion of irrigation activities in September, the influx of water back into the farmlands effectively ceased, rendering it impossible to monitor pollutants in the Sixth Drainage Ditch. Consequently, only the concentrations of various pollutants in the drainage ditch during the remaining six months of the monitoring period were assessed. The pollutant concentrations in the control sections both upstream and downstream of the Sixth Drainage Ditch are illustrated in Figure 4. The criteria for the qualitative evaluation of water quality at cross-sections are shown in Table 1.
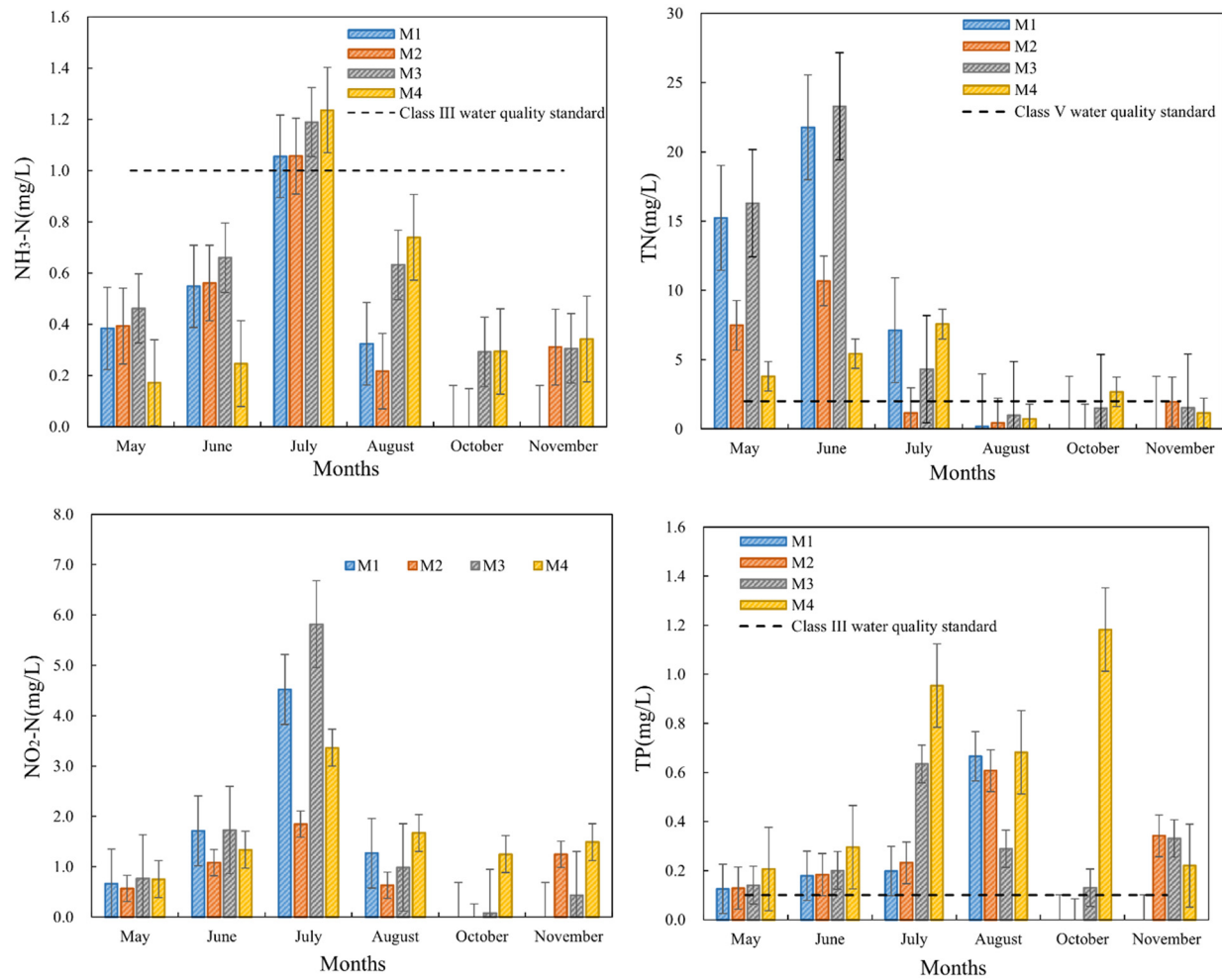
Figure 4. Concentrations of various pollutants at the four control sections of the Sixth Drainage Canal.

Table 1. Qualitative assessment of water quality at cross-sections.

Water Quality Category	Water Quality Status	Characterize Color	Water Quality Functional Categories
I~II water quality	Superior	Blue	Drinking water source primary protection zones, rare aquatic habitats, fish and shrimp spawning grounds, and baiting grounds for young juvenile fish. Shrimp spawning grounds, baiting grounds for juvenile fish, etc.
Class III water quality	Favorable	Green	Drinking water source secondary protection areas, fish and shrimp wintering grounds, migratory pathways, aquaculture areas, swimming areas and other areas. channels, aquaculture areas, swimming areas, etc.
Class IV water quality	Light pollution	Yellow	General industrial water and recreational water not in direct contact with humans.
Class V water quality	Moderate pollution	Orange	Water for agriculture and general landscaping.
Inferior V water quality	Heavy pollution	Red	Poor functionality except for local climate regulation.

According to Figures 3 and 4, it can be observed that there is a close relationship between the variation in the pollutant concentration in the water and the flow rate. This relationship exhibits a certain seasonality, with pollutant concentration peaks occurring earlier than flow rate peaks. The monthly TN load distribution increases rapidly with the increase in the field drainage volume, whether during the crop irrigation period or the

winter irrigation period. In June, the TN concentration is at its maximum, and its peak precedes the flow rate peak. The NO_2-N, NH_3-N, and TP concentrations at all sections peak in July, showing consistent characteristics, with the concentrations gradually rising as the drainage ditch flow increases. The highest TN concentration appears in June, with TN concentrations exceeding 2 mg/L in the months of May to July, classifying the water as worse than Class V. From July to September, the TN concentrations range from 0.186 to 0.984 mg/L, classifying it as Class II to Class IV water. The changes in the NH_3-N and TP concentrations follow a similar pattern, with insignificant differences in the TN concentration between the upstream and downstream monitoring sections during the same time period. In July, the NH_3-N concentrations at all sections exceed the limits for Class III water quality, with the TP concentrations ranging from 0.005 to 0.954 mg/L.

In October and November, the M1 monitoring section has no flow, and the NO_2-N and TP concentrations at M2, M3, and M4 are much lower than those from May to September. The M2 and M3 sections exhibit similar characteristics in the change in the NH_3-N and TP concentrations, gradually increasing with the field drainage concentration and then decreasing. Before planting, a significant amount of nitrogen and phosphorus fertilizers are applied as basal fertilizers for crops. The period from May to June is the growth phase for crops, and additional fertilization is carried out to increase the yield, leading to an increase in pollutant concentrations in the water in June. During the irrigation period in July and August, the pollutant concentrations decrease due to dilution from field drainage and precipitation and the absorption and decomposition of pollutants by plants in the drainage ditch. In September, when irrigation in the region ceases, there is a significant reduction in the drainage volume, resulting in a decrease in various pollutants from field runoff and a subsequent decrease in pollutant concentrations in the water. In November, due to winter irrigation and the decay of aquatic plants, pollutants like nitrogen and phosphorus are released into the water and sediment, causing pollutant concentrations to rise again.

3.2. Pollution Load Modeling

Upon incorporating the water quality monitoring data and flow data for the monitoring point within the Sixth Drainage Ditch section, the LOADEST model proceeds to identify the most suitable regression model from a range of candidate models (1–9). This selection is facilitated by the automatic selection option, which is grounded in AIC and SPCC criteria. Following model optimization, load regression equations for NH_3-N, NO_2-N, TN, and TP pollutants are derived, and their effectiveness is assessed. The parameter details for these regression equations pertaining to NH_3-N, NO_2-N, TN, and TP pollutants are provided in Table 2.

Through the utilization of flow and water quality data from each monitoring section, we carried out parameter calibration for the pollution load regression equations. Table 2 provides the coefficient of determination (R^2) for these regression equations, serving as a pivotal indicator of the model's goodness of fit. Ranging from 0 to 1, R^2 signifies the extent to which the regression model aligns with the data, with higher values indicating a stronger fit and reduced disparities between the predicted and observed values. In the LOADEST model context, an R^2 value exceeding 0.8 is conventionally seen as a confirmation that pollutants adhere to the estimation model, establishing a solid degree of reliability with statistical significance ($p < 0.05$). When R^2 exceeds 0.9, it highlights an exceptionally high level of fitting quality in the estimation model ($p < 0.01$), underscoring its effectiveness in reflecting water pollution load.

The data in Table 2 illustrate the determination coefficients (R^2) for the pollutant load regression equations covering NH_3-N, NO_2-N, TN, and TP across the four monitoring sections within the Sixth Drainage Canal. These coefficients range from a minimum of 72.42% to a maximum of 94.4%. These values signify that the pollutant load regression equations exhibit reasonably strong fits. Specifically, the R^2 values for both the M1 and M2 sections exceed 0.8, indicating a high degree of reliability in the estimation model. While the determination coefficient for the TN load regression equation is relatively low in the M3

section, the others all surpass the 0.8 threshold. In the case of the M4 section, the NH_3-N load regression equation is the only exception, with an R^2 above 0.8, while the others fall within the range of 0.7 to 0.8. In summary, the pollutant load regression equations selected by the LOADEST model demonstrate a notable level of effectiveness, making them well suited for estimating pollutant loads within the Sixth Drainage Canal.

Table 2. LOADEST model parameters for daily pollutant loads in various sections of the Sixth Drainage Ditch.

Section	Pollutants	a0	a1	a2	a3	a4	a5	a6	R^2
M1	NH_3-N	−4.050	0.922	0.257	/	/	/	/	82.12
	NO_2-N	−5.644	0.885	1.322	−2.752	−1.266			94.4
	TN	−5.413	1.099	−0.066	3.436	0.538	0.064	13.115	92.42
	TP	13.397	2.625	−0.956	1.538	12.758	−0.915	−24.268	89.14
M2	NH_3-N	−1.541	0.885	1.475	/	/	/	/	85.82
	NO_2-N	−2.036	1.333	−1.776	/	/	/	/	87.37
	TN	−0.434	1.092	0.139	0.942	1.055	/	/	89.61
	TP	−3.423	0.924	−1.567	/	/	/	/	80.08
M3	NH_3-N	−1.650	0.863	0.007	1.144	−1.098	−0.049	−6.841	81.92
	NO_2-N	−2.499	0.944	−0.038	0.952	−0.449	−0.808	0.506	90.23
	TN	−0.991	1.010	0.057	0.946	1.088	−0.622	−0.049	73
	TP	−3.434	1.730	0.136	−0.581	0.041	−3.148	−6.622	89.42
M4	NH_3-N	−2.993	1.330	0.452	0.515	−0.980	−1.550	−6.128	86.04
	NO_2-N	−2.304	0.591	0.305	0.702	0.541	−1.059		72.42
	TN	−0.831	1.306	0.122	0.343	0.857	−1.323	−1.744	78.24
	TP	−4.511	1.682	−3.209	/	/	/	/	73.21

3.3. Analysis of Spatiotemporal Variation Characteristics of Pollutant Loads

3.3.1. Analysis of Temporal Variation Characteristics of Pollutant Loads throughout the Year

The flux variations in the pollutants (NH_3-N, NO_2-N, TN, and TP) for various sections of the Sixth Drainage Ditch from May to November 2021 are shown in Figure 5.

As depicted in Figure 5, the trends in NH_3-N, NO_2-N, TN, and TP exhibit a noteworthy consistency across the same monitoring sections. The pollutant loads in the upstream M1 and M2 sections experience a progressive increase from May to June, culminating in peak values in June, followed by a steady decline in the subsequent months. In October, due to the absence of flow within the channel, the pollutant load drops to zero. However, during November, corresponding to the winter irrigation period, the heightened channel drainage leads to a resurgence in pollutant loads. The M3 and M4 sections in the middle and lower reaches witness a similar monthly increase in pollutant loads from May to July, reaching their zenith in July, and subsequently declining as the months progress. This period coincides with the growth phase of crops in the irrigation area and encompasses the prime time for farmland irrigation, featuring frequent agricultural activities such as irrigation and fertilization. In the upstream, where wheat and corn are the predominant crops, the peak pollutant load in June results from the final round of irrigation and fertilization for wheat, coinciding with the initial irrigation and fertilization of corn. In the downstream section, where corn is the primary crop, July is the peak period for irrigation and fertilization activities. Beyond July, agricultural practices gradually diminish, leading to a decline in pollutant loads. During the winter irrigation period in November, nitrogen and phosphorus elements that remained underutilized in farmland drainage make their way into the ditch as farmland water recedes. Furthermore, nitrogen and phosphorus elements released from the sediment in the ditch contribute to an increase in pollutant loads within the channel.
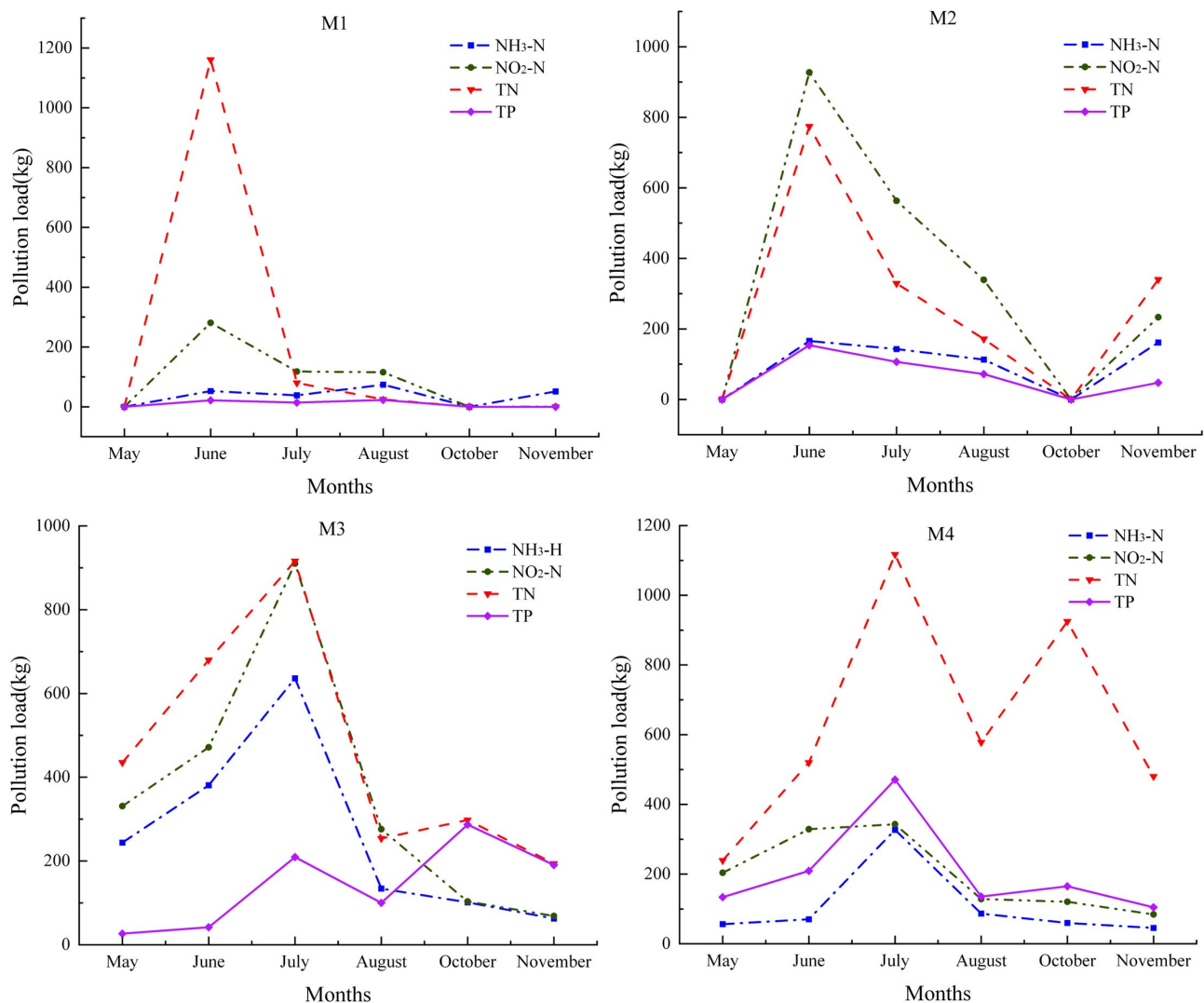
Figure 5. Changes in pollutant fluxes for each section of the Sixth Drainage Ditch.

3.3.2. Analysis of Spatial Variation Characteristics of Pollutant Loads

The LOADEST model was employed to establish a statistical correlation between pollutant loads and flow rates within the Sixth Drainage Ditch. Subsequently, daily flow data were utilized to estimate pollutant loads in this ditch. The cumulative monthly loads of NH_3-N, NO_2-N, TN, and TP from May to November 2021 were aggregated to derive the annual pollutant loads for each section in 2021. The results are presented in Figure 6.

The four sections within the Sixth Drainage Ditch exhibit varying degrees of pollution from different pollution sources, and the output loads display spatial differences based on environmental capacity. Notably, the TN load within this domain surpasses that of the TP. The spatial distribution characteristics of the TN and TP loads gradually intensify from upstream to downstream. M4 demonstrates the highest TN and TP loads, amounting to 3859 kg and 1219 kg, respectively. In stark contrast, M1 presents the smallest load, with 1266 kg and 58 kg for the TN and TP, respectively. Similarly, the spatial distribution trends for NH_3-N and NO_2-N follow an initial increase followed by a decrease. The M3 section exhibits the most substantial NH_3-N and NO_2-N loads, totaling 1457 kg and 2160 kg, respectively. In contrast, M1 records the smallest load, with 216 kg for NH_3-N and 514 kg for NO_2-N. The sections with higher pollutant loads are primarily situated within M3 and M4.
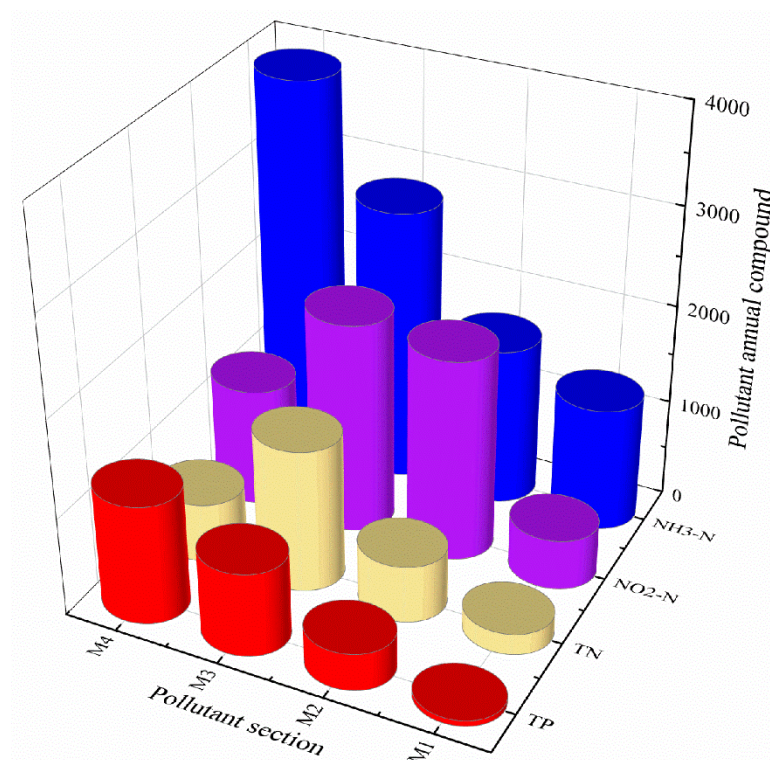
Figure 6. Annual composite chart of pollutants.

Based on field surveys and village visits, the analysis underscores that the channel flow stands as one of the principal factors influencing the results of load simulation. This flow is notably shaped by the irrigation and fertilization processes involved in crop cultivation, contributing to periodic fluctuations in the channel's water levels. In the upstream M1 monitoring section, characterized by a relatively small, controlled drainage basin area, the section's drainage flow remains limited. The midstream monitoring sections, M2 and M3, share similar drainage flow patterns. Contrastingly, in the downstream M4 section, spanning from mid-June to late August, several locations employ water pumps to extract water from the ditch, resulting in lower downstream flow compared to upstream M3. M3 and M4, situated in Baofeng Town, exhibit a higher population density, increased production activities, and greater discharge of domestic, industrial, and livestock wastewater. As pollutants from the upstream regions are transported downstream by the water flow, this leads to an amplified pollution load in the downstream areas. The relatively elevated NO_2-N levels at M2, second only to M3, are attributed to the predominant cultivation of vegetables by the surrounding farmers. As vegetables have a shorter growing season, they require an annual fertilizer application of approximately 170 kg per mu, which exceeds the typical 90 kg per mu used for grain crops. The primary reason for the heightened pollution load at the downstream M3 monitoring section, as compared to M4, is the frequent use of water pumps to extract water for irrigation, leading to a reduction in the channel water volume from mid-June to late August.

4. Discussion

This study delves into the variations in flow rates and pollutant concentrations within the monitoring sections of the Sixth Drainage Channel. The results indicate a strong consistency between the drainage water pollution process and the agricultural irrigation drainage cycle, with the Sixth Drainage Ditch primarily affected by agricultural irrigation drainage and non-point source pollution. Using the LOADEST statistical model, pollutant loads for the Sixth Drainage Ditch in the Ningxia Yellow River Irrigation District were estimated. Pollutant loads for the four sections increase with the water usage during the

crop irrigation period. The pollutant load peaks at the upstream M1 and M2 sections occur earlier compared to the downstream M3 and M4 sections. However, as pollutants accumulate downstream with the flow, the downstream sections exhibit larger pollutant load peaks and greater total pollutant loads. This aligns with the findings of Yang Lihui and others [24] who found that agricultural drainage water pollution in the Yinchuan North Irrigation District primarily occurs during the irrigation period, and there is a significant positive correlation between the agricultural pollution load and drainage volume, consistent with the results of this study.

Currently, it is challenging to monitor pollutant concentrations in agricultural drainage ditches in real time, resulting in limited actual data on pollutant concentrations. The LOADEST model is suitable for situations with limited actual pollutant concentration data and continuous daily flow data. It has lower data requirements, effectively addressing the issue of limited pollutant concentration data in agricultural drainage ditches. Although the LOADEST model has lower data requirements, it is quite reliable in simulating and estimating pollutant loads. The model relies on statistical methods and uses regression equations to estimate pollutant loads, making it a practical approach. By validating the feasibility of the LOADEST model in the Ningxia Yellow River Irrigation District and conducting pollutant load estimates, this study provides strong support for water quality management in the region. It also offers information for similar geographical and environmental conditions, serving as a reference for research and management in other areas.

The relationship between pollutant loads and discharge is crucial for environmental management. By studying the correlation between the two, we can identify pollution sources, predict pollution events, and formulate effective pollution control strategies, thereby achieving more precise water resource management. This not only helps reduce adverse impacts on water bodies but also provides a scientific basis for the development of sustainable environmental policies, ensuring the effective maintenance of and improvement in water quality [23]. Using the LOADEST model, Song Fangfang [25] constructed pollutant flux regression equations, calibrated and validated regression equation parameters, estimated the monthly average flux of COD, NH_3-N, TN, and TP in Zhaojia Creek, and proposed a water quality assessment method based on pollutant flux, laying the groundwork for runoff pollution control measures in Zhaojia Creek. In this study, we established a pollutant flux regression equation for drainage ditches in the Ningxia Yellow River Irrigation Area based on the LOADEST model. Using daily flow data, we estimated the flux changes of pollutants (NH_3-N, NO_2-N, TN, and TP) at various cross-sections of the Sixth Drainage Ditch from May to November 2021, obtaining monthly and annual loads for each pollutant. The results emphasize the seasonal variability of pollutant loads and explore the correlation between pollutant loads and discharge. During the crop irrigation period, pollutant loads continue to rise, and when irrigation ceases, pollutant loads decrease. By investigating the temporal and spatial variations in pollutant loads, we aim to provide fundamental data and critical information for the development of more scientific, precise, and sustainable water resource management and pollution control strategies in the drainage ditches of the Ningxia Yellow River Irrigation Area.

Future research should consider comprehensive data, model sensitivity analysis, watershed integrated management, and stakeholder involvement to address the limitations and enhance the practical applicability of the research. Understanding the changes and trends in pollutant loads in agricultural drainage ditches is crucial for developing more effective pollution control measures, improving agricultural drainage systems, reducing the negative impact on water bodies, and promoting sustainable agriculture and water resource management.

5. Conclusions

This study focuses on the Ningxia Yellow River Irrigation Area, with the Sixth Drainage Canal selected as the representative drainage channel for investigation. The research involves determining the pollutant concentrations at four monitoring sections to explore the

characteristics of flow and pollutant concentration variations in the study area. Additionally, this study aims to analyze the spatiotemporal changes in pollutant loads. The ultimate goal is to provide comprehensive and in-depth foundational data and theoretical support for improving water environmental quality in the Ningxia Yellow River Irrigation Area. The key findings are summarized as follows:

(1) The flow rate and pollutant concentration at various sections of the Sixth Drainage Ditch exhibit a positive correlation and show some seasonal variations. For the same monitoring section, the trends for different pollutants are relatively consistent, all displaying an increase followed by a decrease as irrigation water usage increases. The peak concentrations of pollutants at the M1 and M2 monitoring sections occurred in June, with total pollutant loads of 1515.77 kg and 2020.8 kg, respectively. For the M3 and M4 monitoring sections, the peak pollutant concentrations were observed in July, with total pollutant loads of 2671.5 kg and 2258.07 kg, respectively.

(2) Based on the LOADEST model, the loads of NH_3-N, NO_2-N, TN, and TP were calculated for the four monitoring sections of the Sixth Drainage Ditch. The coefficient of determination (R^2) for the pollutant load regression equations ranges from a minimum of 72.42% to a maximum of 94.4%, indicating a good fit of the pollutant load regression equations. The regression equations selected by the LOADEST model are suitable for estimating the pollutant loads in the Sixth Drainage Ditch.

(3) In the drainage area of the Sixth Drainage Ditch, the TN load surpasses that of the TP. The spatial distribution of the TN and TP loads exhibits a gradual increment from upstream to downstream, with M4 registering the highest TN and TP loads. The spatial distribution characteristics of NH_3-N and NO_2-N both exhibit an initial increase followed by a decrease. At the M3 section, the maximum loads for NH_3-N and NO_2-N were observed, reaching 1457 kg and 2160 kg, respectively, while the M1 section had the minimum values at 216 kg for NH_3-N and 514 kg for NO_2-N. The sections with comparatively higher pollutant loads are located at M3 and M4.

(4) The LOADEST model offers strong operability, simplicity in modeling, and relative ease in data acquisition. It only requires water quality and flow data for calculating the pollutant loads. Through investigations and analyses, it was found that agricultural practices significantly influence the variations in the pollutant loads in the Sixth Drainage Ditch. Therefore, it is recommended that the relevant authorities provide guidance to farmers on fertilization practices, encourage the use of balanced and organic fertilizers, and minimize the risk of non-point source pollution caused by excessive fertilization.

References

1. Xia, J.; Diao, Y.X.; She, D.X. Analysis on ecological security and ecological carrying capacity of water resources in the Poyang Lake Basin. *Water Resour. Prot.* **2022**, *38*, 1–8+24.
2. Li, Q.K.; Li, H.E. Preliminary Framework for Nonpoint Source Pollution Research in the Yellow River Basin. *Yellow River* **2010**, *32*, 131–132+135.
3. Chen, Y.Y.; Wang, Y.S.; Yi, J. Situation and Cause of Agricultural Non-point Source Pollution in Henan in Irrigation District of the Lower Yellow River. *Chin. Agric. Sci. Bull.* **2011**, *27*, 265–272.
4. Xu, A.Q.; Cao, J.Y.; Xia, Y.C. Research on the status and control counter measures of agricultural non-point source pollution in Yuhang Distinct, Hang-Zhou. *Environ. Pollut. Control* **2015**, *37*, 106–110.
5. Guo, H.P.; Zhang, W.; Song, W.H.; Wen, J. Study on Methods of Agricultural Non-point Source Pollution. *Environ. Sci. Manag.* **2018**, *43*, 135–138.
6. Ma, R.; Chen, K.; Guo, Y.Y. Spatial and Temporal Distribution Characteristics of Agricultural Non-Point Source Nitrogen Pollution in Shiwenhe Basin Based on SWAT Model. *Soil Water Conserv. China* **2020**, *07*, 61–64.
7. Dong, X.; Zhou, H.H. Calculation and Study of Total Nitrogen Inflow in the Tributaries of Shanxi Reservoir. *Zhejiang Hydrotech.* **2017**, *45*, 22–24.
8. Li, N.; Sheng, H.; He, C.J. Pollutant Fluxes Estimation for Baoxiang River, Dianchi Lake by Using LOADEST Model. *J. Basic Sci. Eng.* **2012**, *20*, 355–366.
9. Qian, Y.; Migliaccio, K.W.; Wan, Y. Trend Analysis of Nutrient Concentrations and Loads in Selected Canals of the Southern Indian River Lagoon, Florida. *Water Air Soil Pollut.* **2007**, *186*, 195–208. [CrossRef]
10. Pointer, B.; Harned, D.A.; Harden, S. Estimation of Nitrogen Loads to Two Impaired Reservoirs in the Piedmont Region of North Carolina Using LOADEST and SPARROW Models, 1997–2008. AGU Fall Meeting Abstracts. 2010, p. H41E-1122. Available online: https://ui.adsabs.harvard.edu/abs/2010AGUFM.H41E1122P/abstract (accessed on 1 December 2023).
11. Duan, S.; Kaushal, S.S.; Groffman, P.M. Phosphorus export across an urban to rural gradient in the Chesapeake Bay watershed. *J. Geophys. Res. Biogeosci.* **2012**, *117*. [CrossRef]
12. Robert, M.H.; James, W.M.; Bruce, J.P. Seasonal and Annual Fluxes of Nutrients and Organic Matter from Large Rivers to the Arctic Ocean and Surrounding Seas. *Estuaries Coasts* **2012**, *35*, 369–382.
13. Toomas, T.; Nõges, T.; Järvet, A. Contributions of DOC from surface and groundflow into Lake Vortsjarv (Estonia). *Hydrobiologia* **2008**, *599*, 213–220.
14. Meng, F.J.; Guo, Y.X.; Xu, G.D. Analysis of Nitrogen and Phosphorus Pollution Flux from Huai River into Hongze Lake Based on LOADEST Model and M-K Test. *Adm. Tech. Environ. Monit.* **2023**, *35*, 17–22.
15. Wang, H.; Ma, W.; Yang, Z. Estimation of base flow nitrogen and phosphorus output flux in Simao River based on digital filtering and LOADEST model. *Water Resour. Prot.* **2023**, *39*, 186–194.
16. Han, X.Y.; Li, C. Present Situation of Water Environment and the Comprehensive Utilization of Water Resources in Ningdong Base. *J. Soil Water Conserv.* **2014**, *6*, 51.
17. Li, C.; Peng, W.; Shen, X. Comprehensive Evaluation of the High-Quality Development of the Ecological and Economic Belt along the Yellow River in Ningxia. *Sustainability* **2023**, *15*, 11486. [CrossRef]
18. Lin, J.B.; Wang, Y.J.; Shen, X. Research on economic driving characteristics of agricultural non-point source pollution in Ningxia. *J. Arid Land Resour. Environ.* **2021**, *35*, 58–65.
19. Yang, G.Q. Study on Temporal and Spatial Distribution and Influencing Factors of Nitrogen in Third Drainage Ditch of Ningxia. Master's Dissertation, Ningxia University, Yinchuan, China, 2022.
20. Kim, J.; Lim, K.J.; Park, Y.S. Evaluation of Regression Models of LOADEST and Eight-Parameter Model for Nitrogen Load Estimations. *Water Air Soil Pollut.* **2018**, *229*, 179. [CrossRef]
21. Gao, J.; White, M.J.; Bieger, K. Design and development of a Python-based interface for processing massive data with the LOAD ESTimator (LOADEST). *Environ. Model. Softw.* **2021**, *135*, 104897. [CrossRef]
22. Yan, C.A.; Du, Z.P.; Yan, B. Spatial Pattern Analysis of Nitrogen and Phosphorus Losses in Baoxiang River Watershed of Dianchi Lake. *Res. Environ. Sci.* **2020**, *33*, 2695–2704.
23. Yu, Y.; Song, F.; Zhao, Z.J. A Study of Pollutant Loads Variations in Shenzhen River Estuary in Recent Decade. *Acta Sci. Nat. Univ. Pekin.* **2020**, *56*, 460–470.
24. Yang, L.H.; Wang, S.L.; Ruan, B.Q. Evolution of drain-based research of irrigation return flow pollution in Yinbei Irrigation Area. *Chin. J. Eco-Agric.* **2015**, *23*, 1580–1587.
25. Song, F.F. Study on the Estimation of Pollutant Fluxes in Zhaojia Creek Based on LOADEST Statistical Model. Master's Dissertation, Chongqing University, Chongqing, China, 2014.